
Towards realistic statistical models of the grid frequency

David Kraljic^{1,2}

1 Faculty of Electrical Engineering, University of Ljubljana, Slovenia

2 Comcom Trading d.o.o., Ljubljana, Slovenia

david.kraljic@fe.uni-lj.si

Abstract

Increased share of renewable sources of energy in a power grid leads to larger deviations in grid frequency from the nominal value resulting in more challenging control and its modelling. In this paper we focus on the grid frequency for the power system of Great Britain because the large share of renewables makes it a template for other power grids in the future and because it exhibits peculiar statistical properties, such as long-term correlations in fluctuations, periodicity, and bi-modal distribution of the grid frequency. By modifications of the swing equation and the underlying noise statistics, which we justify qualitatively and quantitatively, we reproduce these peculiar statistical properties. We apply our model to a realistic frequency response service and show our predictions outperform a standard swing equation model.

1 Introduction

The integration of renewable sources of energy into power grids is an ongoing trend which is mostly driven by an attempt to reduce the emissions of green-house gases during electricity production. The most prominent renewable sources are wind and solar power which are by their nature fluctuating and uncontrollable. High wind and solar share of power generation are typically associated with low effective inertia of the grid which leads to challenges in integrating them into a power system. Power grid with a significant share of renewables is susceptible to larger deviations in the grid frequency [18] which leads to increase in procurement of reserve and ancillary services aimed at stabilising the grid. In recent years, due to the increased share of renewables, the typical size of deviations has been increasing [18], thereby increasing the probability of outages.

Realistic and detailed models of the grid frequency are therefore needed for future-proofing the grid. Modelling of the grid frequency underlies, for example, the estimation of the size of reserve and frequency response services that need to be procured as well as the estimation of the usage of assets, income, and risk of providers of such services.

Most models for the grid frequency start with the swing equation [31]. The simplest models assume that fluctuations are adequately described by Gaussian noise [28, 36, 37]. As we will see in later sections, the properties of the ‘random’ process underpinning the fluctuation in grid frequency exhibit a wealth of structure. The most salient feature, the periodicity in the fluctuations, was identified to be caused by trading on the market [29]. Ref. [16] attempts to model these periodic effects, which show in the autocorrelation function (ACF), by the deterministic and periodic imbalance generated by the market

while using Gaussian noise for the stochastic part. This reproduced the initial exponential drop-off of the ACF and the periodic peaks but had a mismatch in the tails and at the centre of the probability density function (PDF) for the grid frequency. Ref. [30] shows that the tails of the PDF for the grid frequency in continental Europe are heavier than Gaussian and finds that sourcing the noise from Lévy stable distributions improves the fit in the PDF tails, but now over-estimates the tails. Ref. [27] improves on the goodness of fit of the PDF by solving the swing equation with Gaussian noise that has the mean and variance changing slowly with time, leading to q-Gaussian final distributions. Ref. [4] combines this noise model with the insight that the periodicity of the electricity market is responsible for the periodicity of the ACF leading to good quantitative fits to the PDF in the tails and rough qualitative agreement for the ACF.

In contrast to statistical modelling of the grid frequency, one can attempt to predict it for some time frame in the future. Ref. [21] uses predictive models based on nearest-neighbour techniques, whereas Ref. [8] uses auto-regressive models. To avoid purely statistical analysis some properties of the grid frequency fluctuations can be explained by physical reasons. For example, Ref. [35] finds that wind profiles and particular locations of power injection exacerbate the non-Gaussianity of frequency fluctuations.

We select the power system of Great Britain (GB) for studying the statistical properties of grid frequency fluctuations. The GB system is its own synchronous area, so it can be studied in isolation. It is small (compared to e.g. the European Continental Synchronous Area), leading to low inertia, and has a large share of renewable energy¹. Therefore, it can be considered as a template for future grids elsewhere. In this paper we focus on the GB grid frequency but show in the Appendix that similar statistical properties hold also for the European Continental Synchronous Area.

In Section 2 we present the statistical properties of the grid frequency we aim to reproduce with our modelling. In Section 3 we present the physical basis for the modelling, whereas in Section 4 we present a phenomenological model derived from the physical model. In Section 5 we describe the data used in the analyses. In Section 6 we show the results, discuss them, and use them in a real-world application.

1.1 Our contribution

The main contributions of this paper are:

1. We show that the autocorrelation function has a power-law tail and we successfully model it with fractional Gaussian noise. We show that the power-law tail cannot be reproduced by Gaussian or Levy type noise within a simple swing equation framework.
2. We introduce the effective damping factor (related to inertia) and show that it is dependent on the grid frequency. We argue why this is expected for a realistic grid.
3. We show that the probability density function for the grid frequency is double-peaked (bi-modal), which we can successfully reproduce by the frequency dependent effective damping factor.

¹See e.g. <https://www.iea.org/data-and-statistics>

2 The statistical properties of the GB grid frequency

In this section we present the most salient statistical properties of the GB grid frequency which we aim to reproduce in our models. The detailed discussion and modelling are deferred to later sections.

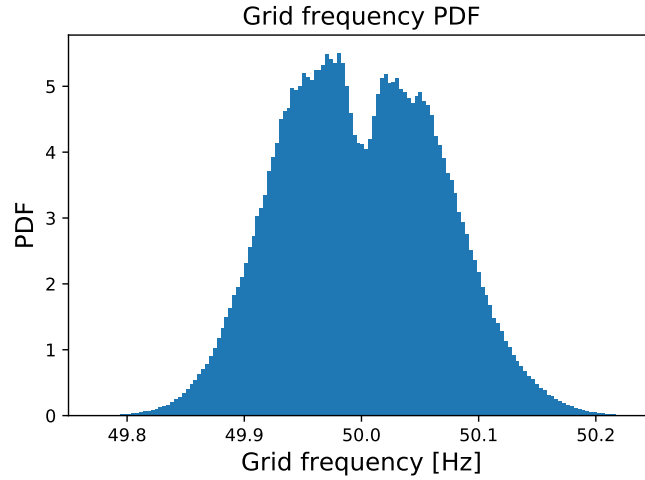


Figure 1. Histogram (PDF) of the GB grid frequency. Note the bi-modal (double-peaked) structure.

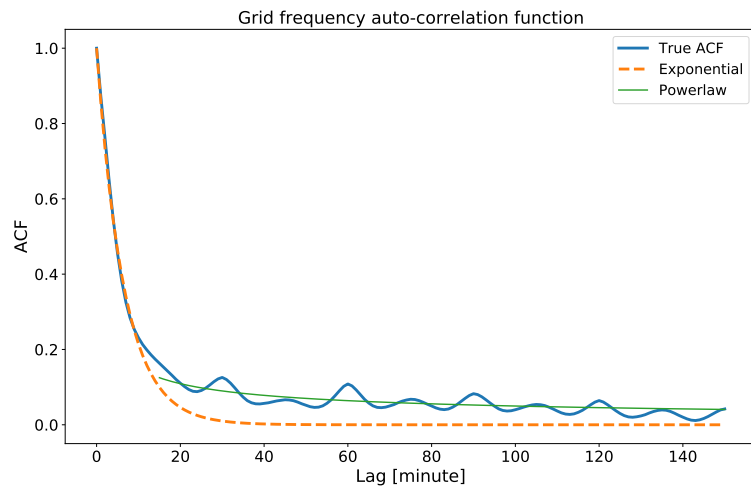


Figure 2. Autocorrelation of the GB grid frequency with lags up to 2.5 hours (150 minutes). Note the quick exponential decay initially followed by a slow power-law-like decrease later.

We would like model the following statistical properties of grid frequency:

1. The autocorrelation function / phase dispersion periodogram
 - (a) The exponential drop for short lags ($\lesssim 10$ min), Fig. 2
 - (b) The periodicity of signal, Figs. 2, 3

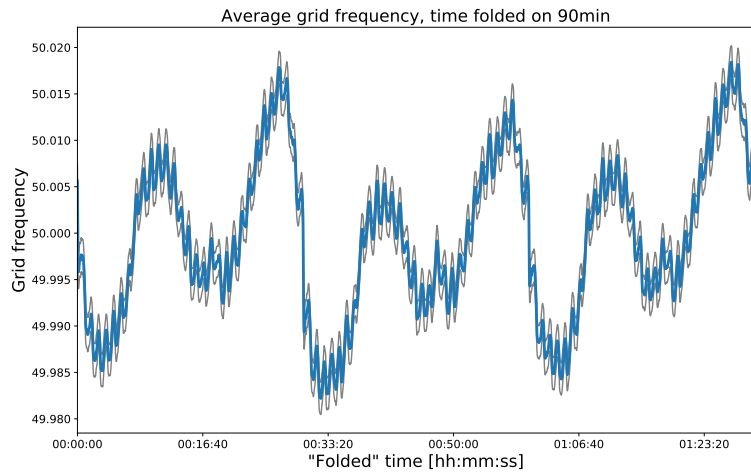


Figure 3. Phase dispersion periodogram – average grid frequency with time ‘folded’ on the period of 90 minutes. This means that, for example, the value for the time label 00:00:12 is the average of grid frequency at times 00:00:12, 01:30:12, 03:00:12, etc.. The two standard deviation bands are plotted in grey.

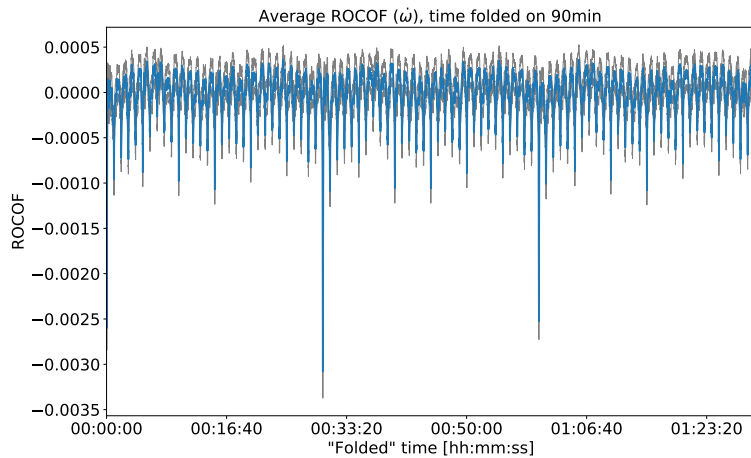


Figure 4. Phase dispersion periodogram – average ROCOF (rate of change of frequency), time ‘folded’ on the period of 90 minutes. The two standard deviation bands are plotted in grey.

- (c) The second-by-second structure (within timescale of exponential drop), Figs. 3, 4
 - (d) The power-law like long range positive correlation, Fig. 2
2. The grid frequency PDF
- (a) The bi-modal (double-peaked) structure, Fig. 1
 - (b) The overall scale of fluctuations

In this contribution we do not focus on modelling the tails of the PDF, as much work has been done in that area, for example in [4, 27, 30].

3 The physical basis for the model

The electric grid consists of many interconnected generators and consumers of power, each of which can be considered as an oscillator(rotator) producing/consuming power at the frequency close to the nominal grid frequency Ω (e.g. 50 Hz). The following analysis closely follows [13]. The phase angle at a rotator i is:

$$\theta_i = \Omega t + \tilde{\theta}_i \quad (1)$$

where $\tilde{\theta}_i$ is the small phase perturbation relative to the whole grid. The power of the rotator is then:

$$P_i = P_i^{\text{dissipated}} + P_i^{\text{accumulated}} + P_i^{\text{transmitted}} \quad (2)$$

where the dissipated power is due to friction, the accumulated power is stored in rotational kinetic energy, and the transmitted power is due to the phase difference between this rotators and the rest of them:

$$P_i^{\text{dissipated}} \propto (\dot{\theta}_i)^2, \quad (3)$$

$$P_i^{\text{accumulated}} \propto M_i \frac{d}{dt} (\dot{\theta}_i)^2, \quad (4)$$

$$P_i^{\text{transmitted}} \propto \sum_{j \neq i} K_{i,j} \sin(\theta_j - \theta_i), \quad (5)$$

where M_i is the rotator moment of inertia, $K_{i,j}$ contains the information on the topology and transmission capacity of the grid (which rotators are connected and the amplitude of the power flow between them), and is symmetric in indices.

Expanding Eq. 2 to first order in perturbations and scaling everything by the moment of inertia results in:

$$\ddot{\tilde{\theta}}_i = p_i - \alpha_i \dot{\tilde{\theta}}_i + \sum_{j \neq i} k_{i,j} \sin(\theta_j - \theta_i) \quad (6)$$

where parameter p_i corresponds to the power of rotator i , α_i to the magnitude of friction, and $k_{i,j}$ to the amount of power that can be transmitted between rotator i and j .

The overall grid frequency ω is the nominal value Ω plus the sum (weighted by the inertia of each rotator) of all individual perturbations:

$$\omega = \Omega + \sum_i M_i \dot{\tilde{\theta}}_i / \sum_i M_i \quad (7)$$

which results in the ‘swing equation’:

$$\dot{\omega} = -\gamma(\omega - \Omega) + \pi(t) \quad (8)$$

where the first restoring term on the RHS contains is pulling the grid frequency towards the nominal value and the second term $\pi(t)$, which perturbs the grid frequency, contains the sum of all generated and consumed powers at each rotator:

$$\pi(t) \propto \sum_i M_i P_i \quad (9)$$

4 The phenomenological model

The physical model of Eq. 8 forms the basis of our modelling of the grid frequency. The physical model contains two unknowns – the perturbation term $\pi(t)$ and the decay factor γ . In this section we consider what determines the values and structure of these unknowns and how they can be empirically modelled.

4.1 The nature of perturbation term $\pi(t)$

In Ref. [27] it is assumed that the powers sum to zero and all that remains is unstructured noise (either of Gaussian or Lévy type) of unknown origin or cause. Specifically, it is assumed that the noise at two different times is uncorrelated. In reality, the powers do not sum to zero at each time instant, as the residual is what drives deviations away from the nominal value, and the term $\pi(t)$ contains a wealth of stochastic and deterministic structure. Of course, the residual of the sum of powers of all rotors can be in first instance approximated as a noise term.

Random part The random part of $\pi(t)$ is caused, for example, by the forecast error in renewable generation, the forecast error in demand, the forecast error of the market regarding imbalance, as well as the effect of faults in the grid (generator tripping). The information on the forecast errors is not available immediately, the error is not rectified immediately (e.g. weather forecast run only a few times daily), and the information does not spread efficiently to all the active participants in the grid (generators, electricity system operators (ESO), traders). This means that the random part of the frequency deviation might exhibit long term dependence.

Non-random part The non-random part of $\pi(t)$ is influenced, for example, by the scheduled decisions of generators, the balancing actions of the ESO, the developments on the power market, the automatic activation of reserve services, generators speculating on the imbalance price, and generators misreporting their physical position. All of the listed things are tied to the common structure – the settlement of imbalances, which is performed at half-hourly intervals in GB, and the market contracts that are structured into half-hourly, 1-hour, 2-hour, and 4-hour blocks. Therefore, we expect deterministic structure to appear and be periodic at these time scales.

The non-random part of $\pi(t)$ also contains responses to the system imbalances by active participants in the grid, which can all be described as terms of the restoring form like $-\gamma^{\text{parti}}(\omega - \Omega)$. For example, the ESO is actively pursuing the balance of the electric system, so its actions can be described by a restoring term. The market, through matching the supply and demand, is also driving the system towards balance and can be described by a restoring term. The primary reserve (a.k.a frequency response) triggered at certain deviations from the nominal frequency and proportional to the size of deviation can be faithfully modelled by a restoring term. Imbalance speculating generators that intentionally produce imbalance to collect payment according to the imbalance price also drive the system towards stability, and consequently frequency towards the nominal value.

Therefore, after removing the terms of the restoring form, the non-random part of the noise term in Eq. 8 can be decomposed into the pure noise term $\xi(t)$ (of unit variance) with the mean $\mu(t)$ and variance $\sigma(t)$ being periodic functions determined by e.g. the periodicity of the market (as in Fig. 3):

$$\pi(t) = \mu(t) + \sigma(t) \cdot \xi(t) \tag{10}$$

4.2 The nature of damping factor γ

The restoring term $-\gamma(\omega - \Omega)$ in Eq. 8 is physical in origin and is determined by the moment of inertia of all the rotators in the grid. In most studies so far the damping factor γ has been assumed to be constant in time, with the exception of Ref. [27]. In fact, due to the varying share of renewable generation in the grid, the moment of inertia of the grid is lower during times of high share of renewable generation. For a review, see

Refs. [12, 19]. Therefore, we expect γ to be a slowly (compared to $\pi(t)$) varying function of time.

The restoring part of Eq. 8 has multiple contributions. As discussed in Sec. 4.1, the active participants in the grid (generators, ESO, traders) also contribute terms of the restoring form. Therefore, the restoring term is described by the overall effective damping factor γ^{eff} including all the contributions. The fact that ESO and reserve services do not react to the smallest deviations in frequency but only if they are above a certain threshold means that the effective damping term γ^{eff} is also likely dependent on the size of deviation resulting in the final model for the grid frequency:

$$\dot{\omega} = -\gamma^{eff}(t, \omega) \cdot (\omega - \Omega) + \pi(t) \quad (11)$$

where $\pi(t)$ now contains only the random and periodic components (Eq. 10). In this paper we will not focus on the time dependence of γ^{eff} but instead on the dependence on ω .

4.3 Modelling the noise $\xi(t)$

The restoring term of Eq. 8 is responsible for the initial exponential decay of the ACF. In the case where γ^{eff} is constant and $\pi(t)$ is uncorrelated Gaussian noise, the model is known as the Ornstein–Uhlenbeck [33] (or Vasicek [34]) model and has an autocorrelation function that decays exponentially with the decay factor γ^{eff} .

Extending such a model by heavy-tailed noise sourced from e.g. a Lévy distribution does not change the exponential drop of the ACF. This can be seen by integrating Eq. 8 and calculating the correlator $\langle \omega(t)\omega(t') \rangle$ [22]. We use the fact that for Gaussian and Lévy type noise $\langle \xi(t)\xi(t') \rangle \propto \delta(t - t')$, where $\delta(t - t')$ is the Dirac delta function. That is, the noise two-point correlation function is non-vanishing only when evaluated at the same instant [14]. Therefore, the long-range dependence seen empirically in the ACF (see Fig. 2) cannot be produced by these types of noise.

Fractional Gaussian noise and long-range dependence Long term dependence, power-law behaviour, and long-term memory processes are frequently described using the fractional Gaussian noise (FGN) [7, 15, 23]. FGN is a generalisation of Gaussian noise for which the correlation of the noise term at two different time instants does not vanish and thus leads to long-range dependence in the ACF. FGN has found application in a variety of fields (e.g. economics [26], hydrology [6], engineering [3]...).

FGN is characterised by a single parameter H , called the Hurst exponent. Standard Gaussian noise is reproduced for $H = 1/2$, $1 > H > 1/2$ results in positive long-range autocorrelations, and $0 < H < 1/2$ results in short-term autocorrelations.

Note that heavy tails can be modelled also within the fractional noise framework, where the underlying noise distribution can be a Lévy stable distribution, thus achieving both the long-range correlations and large point-wise fluctuations [24]. In this contribution we do not focus on the tail part of the PDF, so only consider the more commonly used FGN.

5 The data

The data on GB grid frequency was obtained from the electricity system operator (ESO) in Great Britain [1] and it consists of second by second measurements of the grid frequency floored to three decimal places. We study the data from 2014 to 2020 inclusive.

The data for the European Continental Synchronous Area is obtained from the French ESO [2] and consists of measurements sampled every 10 seconds. We study the data from 2017 to 2020 inclusive.

6 Results and Discussion

6.1 Autocorrelation function: the exponential part

The autocorrelation function has an initial exponential decay and a long-range power-law like part (see Fig. 2). For lags $\lesssim 15$ min the ACF can then be modelled as $\text{ACF}(t) \sim \exp(-\gamma^{eff}t)$. The parameter γ can be extracted by straight line fits on a semi-log plot of the ACF.

The results of the fit is $\gamma^{eff} = (5.5 \pm 0.1 \text{ min})^{-1}$.

6.1.1 Dependence of γ^{eff} on ω

As explained in Sec.4.2 the *effective* damping factor is expected to have a dependence on the value of the grid frequency, i.e. $\gamma^{eff}(\omega)$.

A straightforward approach to estimating $\gamma^{eff}(\omega)$, that is γ^{eff} tabulated by frequency bins, would be to use Eq. 11, select data within the target frequency bin and regress $\dot{\omega}$ on ω and extract γ^{eff} as the coefficient. However, this would lead to biased estimates for the mean and variance of γ^{eff} . The significant and long-term autocorrelation in the residuals (the error term of Eq. 11) leads to biased estimates, which can in principle be corrected for by detailed modelling of the covariance matrix for the error term [10]). The rounding or flooring creates a quantization error of approximate variance $\Delta^2/12$ where Δ is the rounding step size, which can lead to additional biases

Therefore, the parameter γ^{eff} is estimated from the autocorrelation function of ω , where it corresponds to the slope in the log plot of the ACF. We calculate the ACF within a frequency bin by restricting one of the two factors in the ACF to be within the target frequency bin. That is, we study quantity of the form $\langle \omega(t|\omega \in \text{BIN})\omega(t') \rangle$.

We plot the results in Fig. 5 and in Fig. 6. Note that the error in ACF increases with lag distance (as there are fewer independent data points to estimate the ACF). The error increases for bins far away from the nominal value, as the number of data points in those bins is small. Here, special care must be taken as the error in the ACF estimate does not scale as $1/\sqrt{N}$ where N is the number of data points, due to significant autocorrelation which reduces the effective number of data points. We employ a simple correction [5] to obtain the effective number of data points N_{eff} for each estimate of the ACF.

6.2 Autocorrelation function: the power-law part

For the autocorrelations above roughly 15 min the behaviour of the ACF can be described as a power law, $\text{ACF}(t) \sim t^{-\alpha}$. The parameter α can be extracted by straight-line fits on the log-log plot of the ACF.

The result of the fit is $\alpha = -0.5 \pm 0.1$.

Long-range, power-law correlations, can be modelled within the framework of fractional Gaussian noise or fractional Brownian motion. The stochastic noise is described by one parameter, the Hurst exponent H . Hurst exponent H for the noise leads to power-law ACF of t^{2H-2} [25, 32]. Grid frequency power-law fit leads to Hurst exponent of 0.75, suggesting strong long-term dependence. An alternative approach to demonstrate short time exponential decay in the ACF and long time power law is by studying the power spectral density of the process, which we plot in Fig. 7. Power

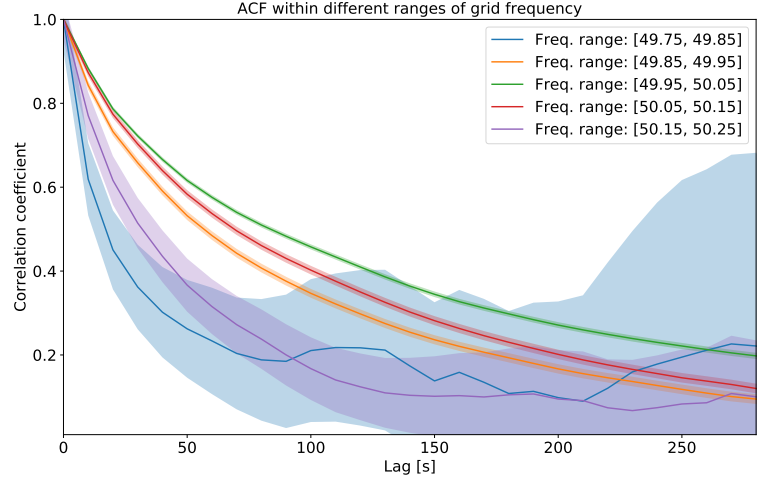


Figure 5. ACF dependence on the grid frequency bin, in the regime where exponential drop-off is a good description.

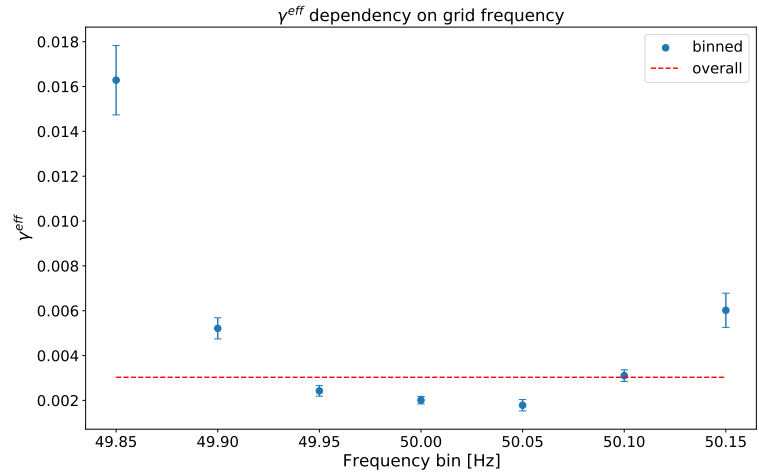


Figure 6. γ_{eff} dependence on the grid frequency bin

spectral density for the swing (OU, Vasicek) type of equation as Eq.8 is described by the following [22]:

$$PSD(k) \sim \frac{\langle \tilde{\pi} \tilde{\pi}^* \rangle}{\gamma^2 + k^2} \quad (12)$$

where k is the inverse of the time scale, γ is related to the decay constant, and $\langle \tilde{\pi} \tilde{\pi}^* \rangle$ is the noise power spectrum. For Gaussian/Lévy noise this is just a constant (Fourier transform of the delta function). However, for fractional noise this term scales as $\langle \tilde{\pi} \tilde{\pi}^* \rangle \sim k^{-2H+1}$ [15, 25]. From the slope (-0.55 ± 0.04) at long times (small k) we show, that the underlying noise process is not Gaussian (slope should be 0) and obtain the Hurst exponent of about 0.75, consistent with estimation from the ACF.

6.3 Simulation results

Equations 8 and 11 are stochastic differential equations, corresponding to a mean-reverting process. If the noise term is Gaussian, then the equations are known as

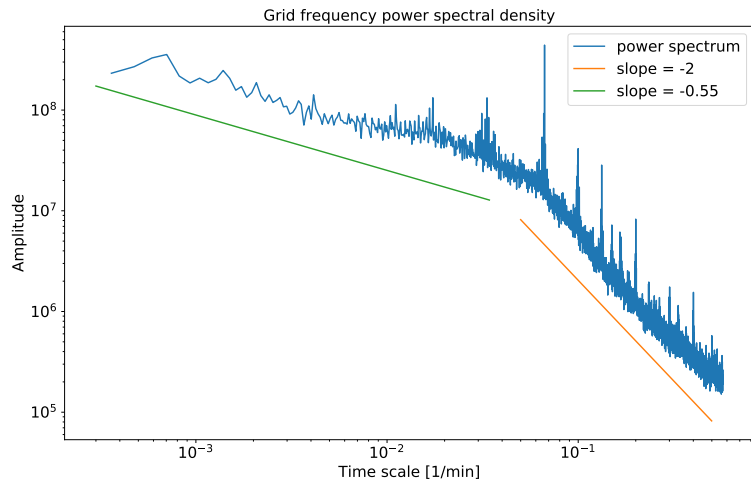


Figure 7. Power spectral density of the grid frequency stochastic process. Note the Brownian/Gaussian scaling (slope=-2) at short times and fractional Brownian scaling at long times. For purely Gaussian noise the spectral density slope should be 0 at long times. Note the peaks due to periodicity.

the Ornstein–Uhlenbeck [33] (or Vasicek [34]) model. Numerical solutions to the equations 8 and 11 are obtained using the Euler–Maruyama method [20]. The equations are solved using NUMPY software package [17], whereas the fractional Gaussian noise is generated using package STOCHASTIC [9].

We compare two models: a simple based on the swing equation, Eq. 8, with Gaussian noise (in essence an OU process), and an elaborate model based on Eq. 11 with fractional Gaussian noise for $\xi(t)$ and ω dependent γ^{eff} with the periodic component of the noise term ($\mu(t)$, $\sigma(t)$) taken from actual data summarised in Fig. 4. For the simple OU model, we chose γ such that the initial exponential drop in the ACF is correctly captured and the overall scale σ of fluctuations is reproduced.

With the elaborate model we can reproduce both the exponential drop-off and power-law tail in the ACF, as well as periodic structure (see Fig. 8). We can also reproduce the over-all scale of fluctuations and the double-peaked structure (Fig. 9), by selecting parameter $\gamma^{eff}(\omega)$ such that the extracted values in Fig. 6 are reproduced in the simulated data.

6.4 Applications

More elaborate modelling of the grid frequency, compared with a simple OU process, should lead to improvements in real-life applications of the models. We choose to show the utility of our model by using it to study a dynamic high-frequency response service. This is, usually, an automatic balancing service provided to an ESO, which triggers at some value higher than the nominal value of the grid frequency, with the consumption power profile proportional to the size of the deviation from the nominal value. That is, the bigger the deviation, the more power is consumed by an asset participating in this service. Thus the distribution of energy requirements, that is, the percentage of the time a certain amount of energy is required to be consumed, is directly linked to the model of the grid frequency.

We take the parameters for a typical GB high-frequency response service², where the

²<https://www.nationalgrideso.com/industry-information/balancing-services/frequency-response-services/firm-frequency-response-ffr>

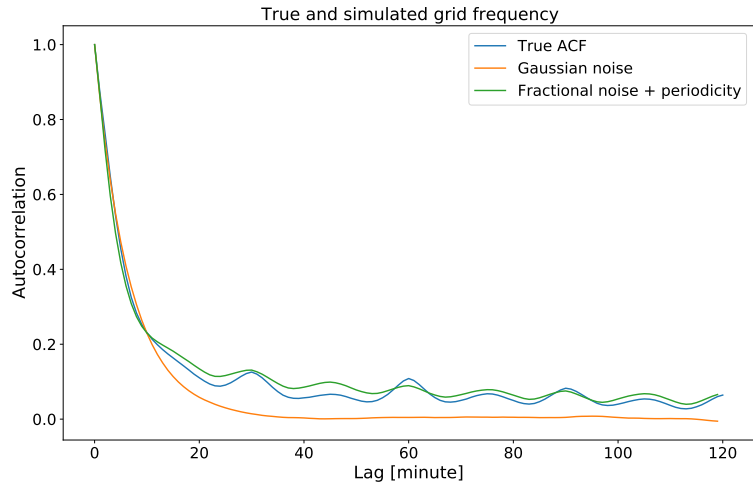


Figure 8. True ACF compared with a simple OU model, and a model based on Eq. 11.

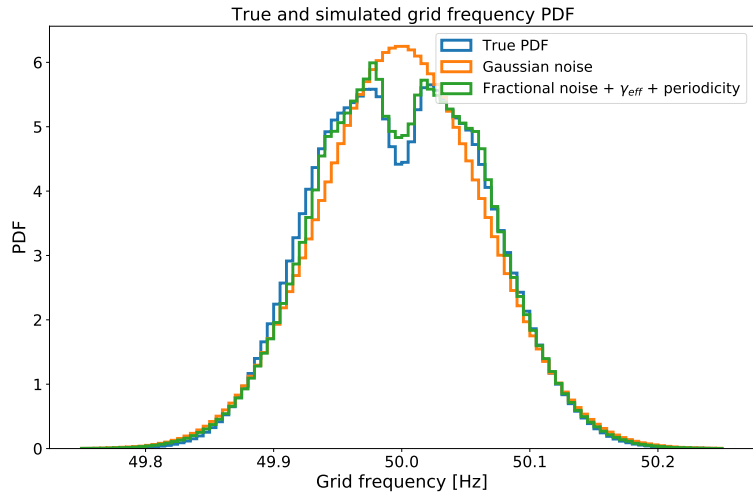


Figure 9. True PDF compared with a simple OU model, and a model based on Eq. 11. Both models match the standard deviation and the mean of the actual frequency data.

response is required within a couple of seconds for deviations above 50.015Hz. In Fig. 10 we plot the CDF of energy requirements for one year. We see that the Gaussian OU process underestimates larger energy requirements, due to the lack of long-term correlations in deviations from the nominal value. This could lead to the wrong sizing of the asset destined for this service, or wrong estimation of expected income. The model we propose contains the long-range dependence and is closer to the true requirement.

7 Conclusions

We study the statistical properties of the grid frequency, focusing on the data for the power system of Great Britain. We show that some curious statistical properties such as the double-peaked probability density function, periodicity, and the long-range power-law dependence in the autocorrelation function, can be modelled successfully by slight modifications of the swing equation or equivalently the Ornstein-Uhlenbeck stochastic process. We show that the effective damping factor is frequency-dependent,

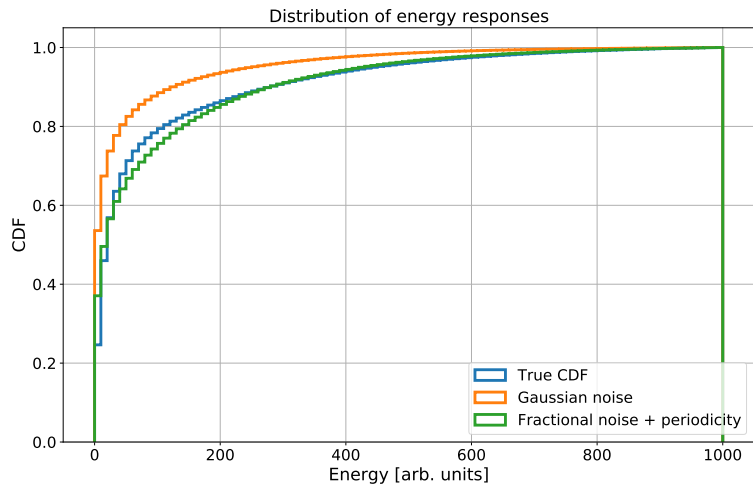


Figure 10. Distribution of energy requirement in a year for a dynamic high frequency response as determined by our models vs true requirement.

which reproduces the double-peakedness. We show that a better description for the underlying noise process, compared to Gaussian, in the swing equation model is fractional Gaussian noise, which due to inherent long term correlations between noise increments reproduces the power-law behaviour in the autocorrelation function. Finally, as an example application, we use our model to determine the distribution of energy requirement for a frequency response service and show its predictions are closer to true values compared to predictions from a standard swing equation model.

Appendix

In this section we show the statistical properties for the European Continental Synchronous Area.

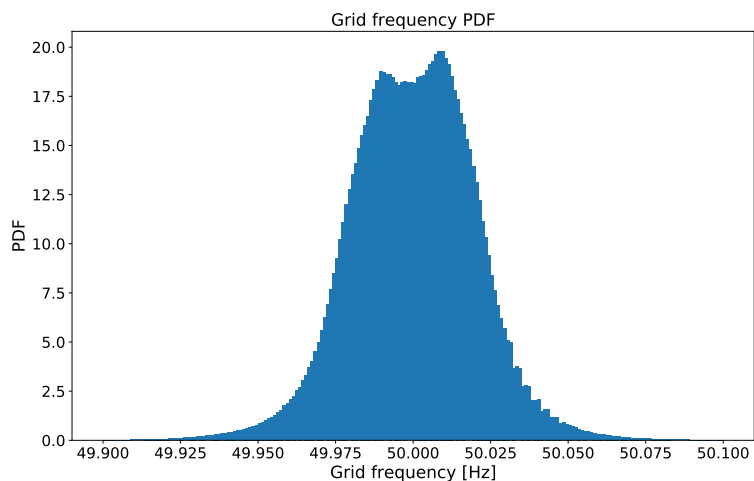


Figure 11. Probability density function for the European grid frequency. Note the slight double-peaked nature. Double-peaked nature is common also in other grids, see e.g. [11].

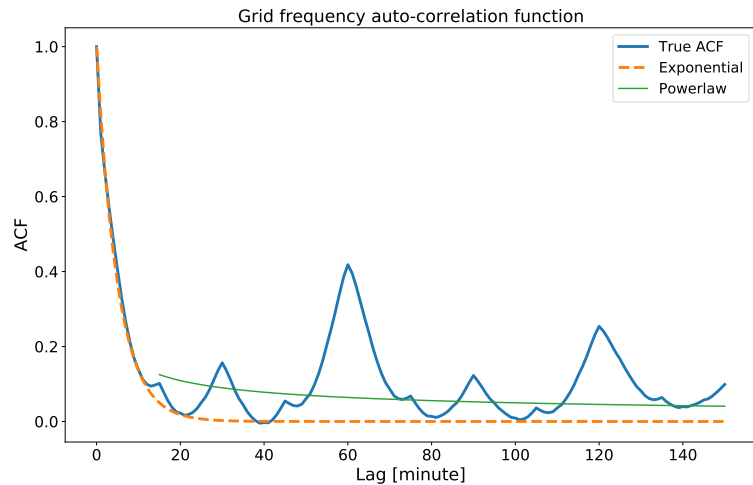


Figure 12. Autocorrelation function for the European grid frequency. Note the strong periodicity.

References

1. *Historic frequency data for great britain*. Available at <https://data.nationalgrideso.com/system/system-frequency-data>.
2. *Historic frequency data from rte*. Available at <https://www.services-rte.com/en/download-data-published-by-rte.html>.
3. P. ADDISON AND A. NDUMU, *Engineering applications of fractional brownian motion: self-affine and self-similar random processes*, *Fractals*, 7 (1999), pp. 151–157.
4. M. ANVARI, L. R. GORJÃO, M. TIMME, D. WITTHAUT, B. SCHÄFER, AND H. KANTZ, *Stochastic properties of the frequency dynamics in real and synthetic power grids*, *Phys. Rev. Research*, 2 (2020), p. 013339.
5. M. BARTLETT, *Some aspects of the time-correlation problem in regard to tests of significance*, *Journal of the Royal Statistical Society*, 98 (1935), pp. 536–543.
6. D. A. BENSON, M. M. MEERSCHAERT, AND J. REVIELLE, *Fractional calculus in hydrologic modeling: A numerical perspective*, *Advances in Water Resources*, 51 (2013), pp. 479–497. 35th Year Anniversary Issue.
7. J. BERAN, *Statistics for long-memory processes*, vol. 61, CRC press, 1994.
8. A. BOLZONI, R. TODD, A. FORSYTH, AND R. PERINI, *Real-time auto-regressive modelling of electric power network frequency*, in *IECON 2019 - 45th Annual Conference of the IEEE Industrial Electronics Society*, vol. 1, 2019, pp. 515–520.
9. CHRISTOPHER FLYNN, *stochastic 0.6.0*. <https://stochastic.readthedocs.io/en/stable/index.html>.
10. D. COCHRANE AND G. H. ORCUTT, *Application of least squares regression to relationships containing auto-correlated error terms*, *Journal of the American Statistical Association*, 44 (1949), pp. 32–61.

-
11. X. DENG, H. LI, W. YU, W. WEIKANG, AND Y. LIU, *Frequency observations and statistic analysis of worldwide main power grids using fnet/grideye*, in 2019 IEEE Power & Energy Society General Meeting (PESGM), IEEE, 2019, pp. 1–5.
 12. A. FERNÁNDEZ-GUILLAMÓN, E. GÓMEZ-LÁZARO, E. MULJADI, AND ÁNGEL MOLINA-GARCÍA, *Power systems with high renewable energy sources: A review of inertia and frequency control strategies over time*, Renewable and Sustainable Energy Reviews, 115 (2019), p. 109369.
 13. G. FILATRELLA, A. H. NIELSEN, AND N. F. PEDERSEN, *Analysis of a power grid using a Kuramoto-like model*, European Physical Journal B, 61 (2008), pp. 485–491.
 14. H. FINK AND C. KLÜPPELBERG, *Fractional Lévy-driven Ornstein–Uhlenbeck processes and stochastic differential equations*, Bernoulli, 17 (2011), pp. 484 – 506.
 15. P. FLANDRIN, *On the spectrum of fractional brownian motions*, IEEE Transactions on Information Theory, 35 (1989), pp. 197–199.
 16. L. R. GORJÃO, M. ANVARI, H. KANTZ, C. BECK, D. WITTHAUT, M. TIMME, AND B. SCHÄFER, *Data-driven model of the power-grid frequency dynamics*, IEEE Access, 8 (2020), pp. 43082–43097.
 17. C. R. HARRIS, K. J. MILLMAN, S. J. VAN DER WALT, R. GOMMERS, P. VIRTANEN, D. COURNAPEAU, E. WIESER, J. TAYLOR, S. BERG, N. J. SMITH, R. KERN, M. PICUS, S. HOYER, M. H. VAN KERKWIJK, M. BRETT, A. HALDANE, J. F. DEL R’IO, M. WIEBE, P. PETERSON, P. G’ERARD-MARCHANT, K. SHEPPARD, T. REDDY, W. WECKESSER, H. ABBASI, C. GOHLKE, AND T. E. OLIPHANT, *Array programming with NumPy*, Nature, 585 (2020), pp. 357–362.
 18. S. HOMAN, N. MAC DOWELL, AND S. BROWN, *Grid frequency volatility in future low inertia scenarios: Challenges and mitigation options*, Applied Energy, 290 (2021), p. 116723.
 19. S. C. JOHNSON, D. J. PAPAGEORGIOU, D. S. MALLAPRAGADA, T. A. DEETJEN, J. D. RHODES, AND M. E. WEBBER, *Evaluating rotational inertia as a component of grid reliability with high penetrations of variable renewable energy*, Energy, 180 (2019), pp. 258–271.
 20. P. KLOEDEN AND E. PLATEN, *The Numerical Solution of Stochastic Differential Equations*, vol. 23, 01 2011.
 21. J. KRUSE, B. SCHÄFER, AND D. WITTHAUT, *Predictability of power grid frequency*, IEEE Access, 8 (2020), pp. 149435–149446.
 22. B. LINDNER, *A brief introduction to some simple stochastic processes*, (2010).
 23. B. B. MANDELBROT AND J. W. V. NESS, *Fractional brownian motions, fractional noises and applications*, SIAM Review, 10 (1968), pp. 422–437.
 24. T. MARQUARDT, *Fractional lévy processes with an application to long memory moving average processes*, Bernoulli, 12 (2006), pp. 1099–1126.
 25. F. J. MOLZ, H. H. LIU, AND J. SZULGA, *Fractional brownian motion and fractional gaussian noise in subsurface hydrology: A review, presentation of fundamental properties, and extensions*, Water Resources Research, 33 (1997), pp. 2273–2286.

-
26. S. ROSTEK AND R. SCHÖBEL, *A note on the use of fractional brownian motion for financial modeling*, *Economic Modelling*, 30 (2013), pp. 30–35.
 27. B. SCHÄFER, C. BECK, K. AIHARA, D. WITTHAUT, AND M. TIMME, *Non-Gaussian power grid frequency fluctuations characterized by Lévy-stable laws and superstatistics*, *Nature Energy*, 3 (2018), p. 119.
 28. B. SCHÄFER, M. MATTHIAE, X. ZHANG, M. ROHDEN, M. TIMME, AND D. WITTHAUT, *Escape routes, weak links, and desynchronization in fluctuation-driven networks*, *Phys. Rev. E*, 95 (2017), p. 060203.
 29. B. SCHAFFER, M. TIMME, AND D. WITTHAUT, *Isolating the impact of trading on grid frequency fluctuations*, in 2018 IEEE PES Innovative Smart Grid Technologies Conference Europe (ISGT-Europe), 2018, pp. 1–5.
 30. B. SCHÄFER, D. WITTHAUT, AND M. TIMME, *How decentral smart grid control limits non-gaussian power grid frequency fluctuations*, in 2018 IEEE Conference on Control Technology and Applications (CCTA), 2018, pp. 32–39.
 31. W. STEVENSON AND J. GRAINGER, *Power System Analysis*, McGraw-Hill Education, 1994.
 32. M. TARNOPOLSKI, *On the relationship between the hurst exponent, the ratio of the mean square successive difference to the variance, and the number of turning points*, *Physica A: Statistical Mechanics and its Applications*, 461 (2016), pp. 662–673.
 33. G. E. UHLENBECK AND L. S. ORNSTEIN, *On the theory of the brownian motion*, *Phys. Rev.*, 36 (1930), pp. 823–841.
 34. O. VASICEK, *An equilibrium characterization of the term structure*, *Journal of Financial Economics*, 5 (1977), pp. 177–188.
 35. M. F. WOLFF, K. SCHMIETENDORF, P. G. LIND, O. KAMPS, J. PEINKE, AND P. MAASS, *Heterogeneities in electricity grids strongly enhance non-gaussian features of frequency fluctuations under stochastic power input*, *Chaos: An Interdisciplinary Journal of Nonlinear Science*, 29 (2019), p. 103149.
 36. A. J. WOOD, B. F. WOLLENBERG, AND G. B. SHEBLÉ, *Power generation, operation, and control*, John Wiley & Sons, 2013.
 37. H. ZHANG AND P. LI, *Probabilistic analysis for optimal power flow under uncertainty*, *IET Generation, Transmission & Distribution*, 4 (2010), pp. 553–561(8).